



# Influence of thermal treatment on structure development and mechanical properties of amorphous $\text{Fe}_{73.5}\text{Cu}_1\text{Nb}_3\text{Si}_{15.5}\text{B}_7$ ribbon

A. Gavrilović<sup>a</sup>, L.D. Rafailović<sup>a,b</sup>, D.M. Minić<sup>c</sup>, J. Wosik<sup>a</sup>, P. Angerer<sup>a</sup>, D.M. Minić<sup>d,\*</sup>

<sup>a</sup> CEST Centre of Electrochemical Surface Technology, 2700 Wiener Neustadt, Austria

<sup>b</sup> Physics of Nanostructured Materials, Faculty of Physics, University of Vienna, 1090 Vienna, Austria

<sup>c</sup> Military Technical Institute in Belgrade, 11001 Belgrade, Serbia

<sup>d</sup> Faculty of Physical Chemistry, University of Belgrade, Studentski trg 12, 11001 Belgrade, Serbia

## ARTICLE INFO

### Article history:

Received 4 July 2010

Received in revised form 6 November 2010

Accepted 17 November 2010

Available online 25 November 2010

### Keywords:

Metallic glasses

Nanostructured materials

Focused ion beam microscopy

X-ray diffraction

## ABSTRACT

Ribbon-shaped amorphous samples with the stoichiometric composition  $\text{Fe}_{73.5}\text{Cu}_1\text{Nb}_3\text{Si}_{15.5}\text{B}_7$  prepared by the melt spinning process were annealed at temperatures ranging from 693 K to 1123 K for 1 h under vacuum. In the early annealing stage, the alloy undergoes a specific nucleation process where Cu clusters precipitate from an amorphous matrix. Further heating initiates the partial crystallization of alloy forming the  $\alpha$ -Fe–Si nanocrystallites. Subsequent Vickers hardness tests showed high values depending on the annealing temperature. It was found that the hardening process includes two stages. This behavior correlates well with results of density dislocation calculations. A crystallite size of 10 nm for the  $\alpha$ -Fe–Si particles correlated very well with a maximum hardness of the material.

© 2010 Elsevier B.V. All rights reserved.

## 1. Introduction

Ribbon shaped amorphous alloys are commonly produced by rapid cooling from the melt. Thermally induced crystallization of amorphous alloys often leads to the evolution of nanocrystalline microstructures, which give rise to excellent physical, chemical and mechanical properties. The microstructure is strongly affected by the annealing temperature and annealing conditions, thus a study of its evolution and the understanding mechanisms of nanocrystallization can provide insight for tailoring a functional material of desired properties.

The soft magnetic amorphous alloys have been widely studied for their superior magnetic properties and potential application in power electronic components [1–4]. These materials have many technical advantages over traditional soft magnetic iron alloys: very high permeability, high saturation induction, low coercivity field strengths, low magnetic reversal losses, low eddy current losses and high Curie temperature [8].

The Fe-based glassy alloys such as Finemet<sup>®</sup> ( $\text{Fe}_{73.5}\text{Cu}_1\text{Nb}_3\text{Si}_{13.5}\text{B}_9$ ) and (Fe<sub>73.5</sub>Cu<sub>1</sub>Nb<sub>3</sub>Si<sub>15.5</sub>B<sub>7</sub>) Vitroperm<sup>®</sup> contain small amounts of Cu immiscible with Fe and Nb. Cu and Nb, in spite their small content, significantly affects the crystalliza-

tion process and are responsible for the nanocrystalline structure of these alloys and their desirable soft magnetic properties. Thus, the role of Nb and Cu in nanocrystallization is of great interest. Almost 10 years ago, Ayers et al. [5] found from Extended X-ray Absorption Fine Structure (EXAFS) measurements that Cu clusters were formed in the Fe–Nb–Cu–Si–B alloys of very similar atomic mass compositions during the heat treatment in an early stage of the crystallization process. There was some evidence that these clusters are present even in the as-prepared amorphous alloy. Further heating initiates the formation of  $\alpha$ -Fe–Si nanocrystals in intimate contact with Cu clusters. As the  $\alpha$ -Fe–Si nanocrystals grow, they expel Cu into the phase boundary space. Hono et al. [6,7] suggest a very similar model of Cu clustering in the early stage of crystallization in the Fe–Nb–Cu–Si–B alloys. According to these authors, the initial amorphous phase is a chemically uniform amorphous solid solution. During annealing, Cu clusters are formed in a fully amorphous matrix. Subsequently, the concentration of Cu in the clusters increased. Finally, the FCC–Cu particles were present in direct contact with the  $\alpha$ -Fe–Si grains, but not entirely enveloped within the  $\alpha$ -Fe–Si grains.

The objective of this work was a detailed study of the Cu cluster formation and the crystallization process of the amorphous  $\text{Fe}_{73.5}\text{Cu}_1\text{Nb}_3\text{Si}_{15.5}\text{B}_7$  alloy in the temperature range of 693–1123 K, especially the understanding of the mechanism of development of the nanostructure and how this nanostructure relates to mechanical properties.

\* Corresponding author. Tel.: +381 11 3336 689.

E-mail addresses: [dminic@ffh.bg.ac.rs](mailto:dminic@ffh.bg.ac.rs), [drminic@gmail.com](mailto:drminic@gmail.com) (D.M. Minić).

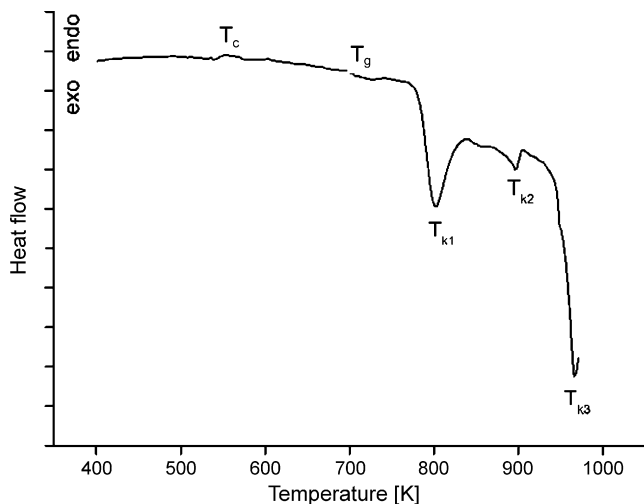


Fig. 1. DSC of as prepared alloy at heating rate  $7 \text{ K min}^{-1}$ .

## 2. Experimental procedures

The amorphous samples with a stoichiometric composition  $\text{Fe}_{73.5}\text{Cu}_1\text{Nb}_3\text{Si}_{15.5}\text{B}_7$  were prepared by rapid cooling of a melt on a rotating disc. The final product was alloy ribbon, 2.5 cm wide and  $35 \mu\text{m}$  thick. The chemical composition of the alloy was examined using energy dispersive X-ray spectroscopy (EDX). Quenched ribbon samples were sealed in quartz tubes under technical vacuum and isothermally annealed for 1 h.

Thermal stability of the samples of alloy was studied by differential scanning calorimetry (DSC) using a DSC-204 C device (Netzsch, Germany) in the temperature range of 400–970 K under Ar atmosphere at a constant heating rate of  $7 \text{ K min}^{-1}$ . A slow heating rate increased sensitivity for detection of smaller exothermic and endothermic changes in DSC.

XRD experiments were performed using an X-Pert powder diffractometer (PANalytical, Netherlands) using  $\text{Cu K}\alpha$  radiation in Bragg–Brentano geometry at 40 kV and 30 mA. The device is equipped with a secondary graphite monochromator, automatic divergence slits, and a scintillation counter. The measurements were conducted in step scan mode at intervals of  $0.05^\circ 2\theta$  with a measuring time of 30 s/step.

The TOPAS V3 general profile and structure analysis software for X-ray powder diffraction data was used for the Rietveld refinement [9].

The Vickers microhardness tests were performed with a microhardness tester MHT-10 (Anton Paar, Austria) with loads of 40 p and 10 s enforcing time. The mean value of seven measurements was used.

The focused ion beam (FIB) technique (Quanta 200, 3D device, FEI Netherlands) was used for cross section preparation. The  $\text{Ga}^+$  ion beam was focused perpendicularly to the surface. An ion current of between 7.1 nA and 0.3 nA was used for cutting of, and between 10 pA and 30 pA for imaging.

Electron backscatter diffraction (EBSD) device also known as a backscattered Kikuchi diffraction (BKD), attached to a Philips XL30 environmental scanning electron microscope (ESEM) was used to verify the phase identification of the Cu grains.

## 3. Results and discussion

DSC analysis of the  $\text{Fe}_{73.5}\text{Cu}_1\text{Nb}_3\text{Si}_{15.5}\text{B}_7$  alloy, at a slow heating rate ( $7 \text{ K min}^{-1}$ ), reveals a series of stepwise structural transformations consisting of endothermic peaks and more pronounced exothermic peaks in the broad temperature range of 400–970 K (cf. Fig. 1).

The broad exothermic maximum in the range of 400–500 K is attributed to the structural relaxation processes. These processes are followed by the Curie temperature around  $T_c = 550 \text{ K}$ , and by the glass transition at temperature  $T_g = 740 \text{ K}$ . Study of  $T_c$  during relaxation combined with some structural data may lead to a better understanding of the process of clustering in the amorphous phase preceding the nanocrystalline structure formation. The process of crystallization involves three well-defined broad asymmetric exothermic peaks ( $T_{k1} = 800 \text{ K}$ ,  $T_{k2} = 896 \text{ K}$  and  $T_{k3} = 966 \text{ K}$ ) indicating a stepwise process of the structural transformations/crystallization of the alloy.

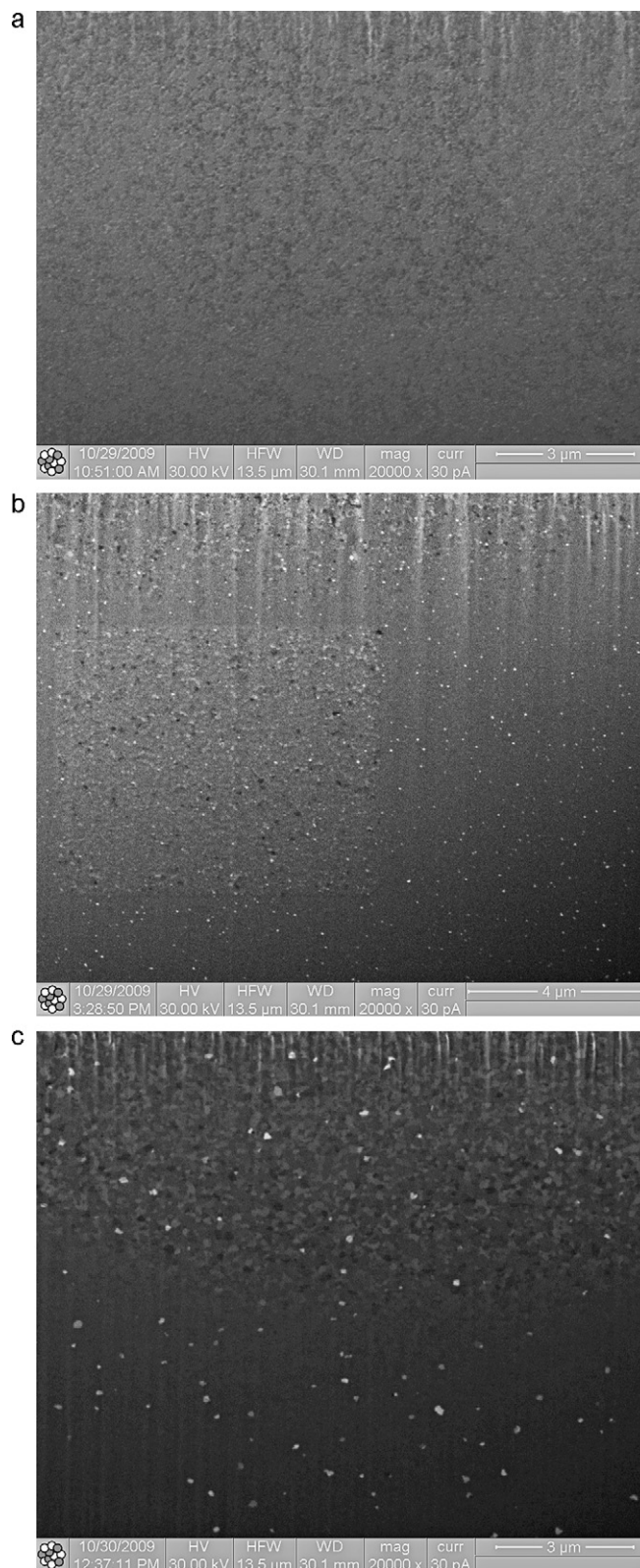
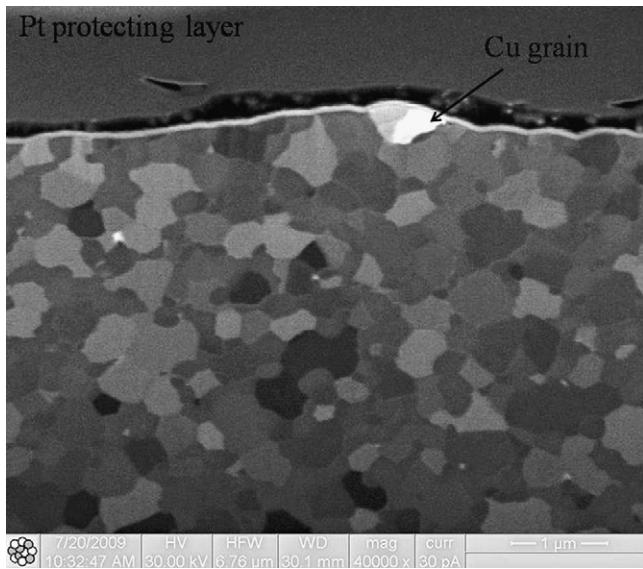


Fig. 2. FIB images of the cross sections of the samples at different stages of annealing: (a) for early annealing stage at 693 K, (b) 753 K, and (c) for the highest annealing temperature 1123 K (1 h dwell each).

XRD investigations of the as prepared  $\text{Fe}_{73.5}\text{Cu}_1\text{Nb}_3\text{Si}_{15.5}\text{B}_7$  alloy confirmed the absence of long range ordering [2]. The FIB imaging conducted in combination with EDX and EBSD analysis confirmed the presence of Cu clusters and the formation of  $\alpha\text{-Fe-Si}$  in the early stages of annealing. Fig. 2a shows that small, embedded Cu



**Fig. 3.** Cross section prepared using FIB technique (30 kV, 30 pA) of the specimen heated at 1123 K for 24 h.

clusters are already present in the amorphous matrix at 693 K. The Cu clusters as can be seen in the FIB image are present in the form of small, bright, spherical particles distributed randomly along the cross section of the sample. The randomly distributed dark shaded regions (Fig. 2b) correspond to the  $\alpha$ -Fe–Si phase.

XRD analysis of the sample annealed at 753 K confirmed that, besides the amorphous fraction of the material, a crystalline  $\alpha$ -Fe–Si phase (FCC structure) was also present as the  $\alpha$ -Fe<sub>3</sub>Si phase (entry PDF 03-065-0146 in ICDD database). Our previous study [2], explains microstructural transformations upon annealing in more detail. It was found that structural composition remained unchanged up to 873 K, when formation of the crystalline phase FeCu<sub>4</sub> (ICDD-PDF 03-065-7002) started. At 923 K, slow dissolution of B and Nb atoms into the Fe matrix led to the formation of two new phases: Fe<sub>16</sub>Nb<sub>6</sub>Si<sub>7</sub> (ICDD-PDF 00-053-0459) and Fe<sub>2</sub>B (ICDD-PDF 00-036-1332). Annealing at 973 K gave rise to two phases in trace amounts: Fe<sub>5</sub>Si<sub>3</sub> (ICDD-PDF 03-065-3593) and Nb<sub>5</sub>Si<sub>3</sub> (ICDD-PDF 03-065-2785).

As it can be seen from Fig. 2b and c the Cu clusters grow at the expense of smaller Cu clusters.

The typical structure of the Fe<sub>73.5</sub>Cu<sub>1</sub>Nb<sub>3</sub>Si<sub>15.5</sub>B<sub>7</sub> alloy, thermally treated at 1123 K for 24 h, as resolved from the FIB image (Fig. 3), consists of small, equi-axial grains with a homogeneous distribution (1  $\mu$ m in size and less). EDX analysis showed that the bright twin-grain in the upper part of the sample surface is Cu enriched.

Since the investigated sample was thermally treated at a comparatively high temperature for quite a long time it is very likely that the Cu clusters, which were not associated with the FCC  $\alpha$ -Fe–Si crystallites in the beginning, grow at the expense of the smaller Cu clusters. This process, called “Ostwald ripening”, is the reason for such high purity of Cu grains. The applied EBSD analysis enabled the phase identification (Fig. 4) and confirmed that randomly distributed Cu enriched grains (bright spots in the micrograph) have FCC structure.

XRD analysis (Fig. 5) shows that heating of the Fe<sub>73.5</sub>Cu<sub>1</sub>Nb<sub>3</sub>Si<sub>15.5</sub>B<sub>7</sub> alloy at 1123 K for 24 h resulted in a formation of the following phases: Fe<sub>3</sub>Si, FeCu<sub>4</sub>, Fe<sub>16</sub>Nb<sub>6</sub>Si<sub>7</sub>, Fe<sub>2</sub>B, Fe<sub>5</sub>Si<sub>3</sub>, and Nb<sub>5</sub>Si<sub>3</sub>. It should be noted that even the relatively large Cu crystallites could not be detected by XRD analysis due to their low amount, on average, in the material (around 1 at.%).

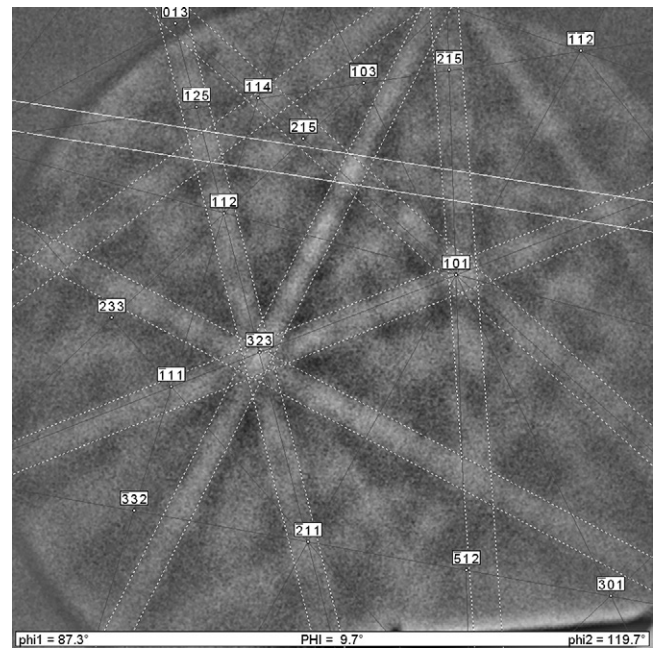


**Fig. 4.** The EBSD image from a Cu grain (corresponding Kikuchi lines).

The Fe–Cu–Nb–Si–B metallic glasses are known to be hard but very brittle materials (Vickers hardness higher than 800 HV) [8]. This is a result of a large number of dislocations accompanied by a reduction in ductility.

XRD data of alloys annealed in the temperature range of 273–1123 K showed that samples with the optimum properties consisted of a nanocrystalline ferromagnetic  $\alpha$ -Fe–Si solid phase (volume fraction 60–65%) with an average grain size of 10 nm embedded in an amorphous matrix. The increased formation of  $\alpha$ -Fe–Si nanocrystallites from the amorphous phase in the temperature range of 753–873 K reduces the content of  $\alpha$ -Fe and Si in the remaining relaxed amorphous matrix. This evidently leads to an increase in hardness (cf. Fig. 6). Furthermore, the particle size of  $\alpha$ -Fe–Si nanocrystallites is comparable to, or smaller than, the thickness of the shear deformation band. For this reason, shear deformation becomes more difficult in the mixed phase alloy consisting of nanoscale  $\alpha$ -Fe–Si embedded in an amorphous matrix,

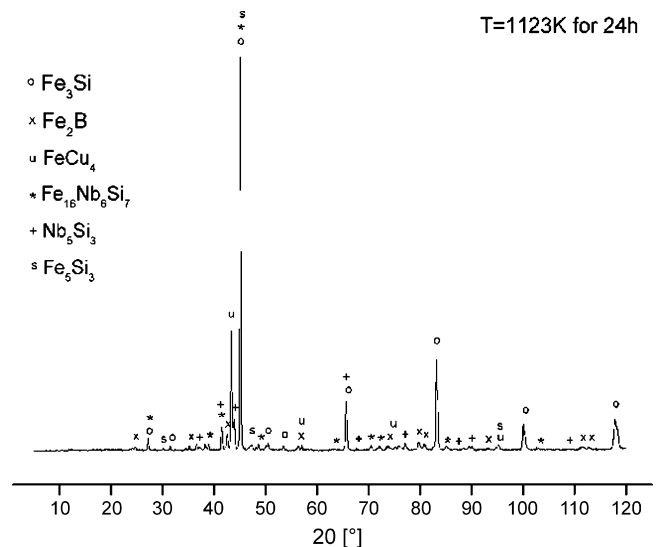


**Fig. 5.** XRD pattern of Fe<sub>73.5</sub>Cu<sub>1</sub>Nb<sub>3</sub>Si<sub>15.5</sub>B<sub>7</sub> alloy sample heated 24 h at 1123 K.

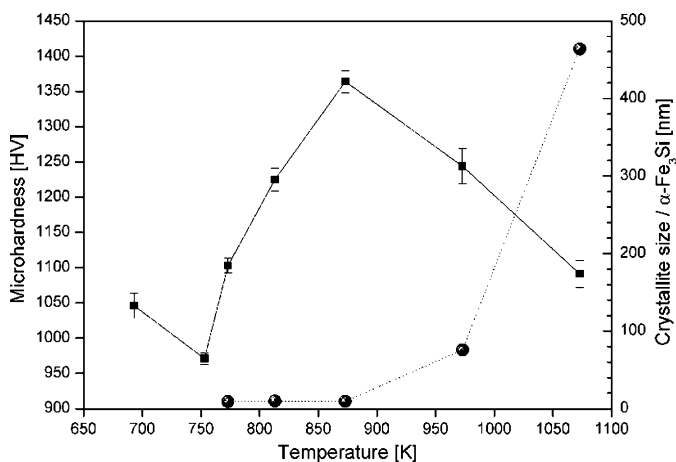


**Fig. 6.** Vickers microhardness of  $\text{Fe}_{73.5}\text{Cu}_1\text{Nb}_3\text{Si}_{15.5}\text{B}_7$  alloy displayed as a function of the annealing temperature and the crystallite size of  $\alpha$ - $\text{Fe}_3\text{Si}$  phase. The measured values of Vickers microhardness are denoted with a square symbol while the crystallite size values as obtained from the Rietveld refinement are denoted with a ball symbol.

than in a single amorphous phase, making the alloy becomes stronger. A homogeneous dispersion of rigid particles free of defects may act as an effective barrier against deformation of the amorphous matrix. The hardening behavior can be dominated by the shear deformation mechanism when  $D_{hkl} < \delta$ , where  $\delta$  is an optimal value [10,11]. In the second stage ( $D_{hkl} > \delta$ ,  $T > 873$  K) when the hardness of the alloy starts to decrease, the hardening behavior is determined by the dislocation density. The corresponding values are presented in Table 4 in our previous work in this journal [2]. It was found, that the microhardness decreases with increased crystallite size ( $D_{hkl} > 10$  nm). The optimum crystallite size of  $\alpha$ - $\text{Fe-Si}$  particles is 10 nm, the optimum annealing temperature is 873 K.

#### 4. Conclusions

In the early annealing stage, the amorphous alloy  $\text{Fe}_{73.5}\text{Cu}_1\text{Nb}_3\text{Si}_{15.5}\text{B}_7$  undergoes a specific nucleation process where Cu clusters precipitate from the amorphous matrix. Further heating initiates partial crystallization through formation of

$\alpha$ - $\text{Fe-Si}$  nanocrystallites in intimate contact with Cu clusters. The presence of Cu clusters and formation of  $\alpha$ - $\text{Fe-Si}$  nanocrystallites at early annealing stages is shown using FIB imaging. The Kikuchi lines analysis confirmed randomly distributed Cu enriched grains with FCC structure. It was found that the hardening process consists of two stages. For  $T < 873$  K and  $D_{hkl} < 10$  nm, the hardening behavior is controlled by a shear deformation mechanism in the amorphous matrix. The nanoscale  $\alpha$ - $\text{Fe-Si}$  particles homogeneously dispersed in the amorphous matrix act as an effective resistance to suppress shear sliding of the amorphous matrix. For  $T > 873$  K and  $D_{hkl} > 10$  nm, the hardening behavior is dominated by the dislocations movement, which in conjunction with appearance of the other crystalline phases upon annealing leads to the decrease of hardness with increase of crystallite size  $D_{hkl}$ . The optimum crystallite size of  $\alpha$ - $\text{Fe-Si}$  particle is 10 nm.

#### Acknowledgements

The investigation is partially supported by the Ministry of Science and Environmental Protection of Serbia within the Project 142025. The work at CEST is supported within the COMET program by the Austrian Research Promotion Agency (Österreichische Forschungsförderungsgesellschaft, FFG) and the government of Lower Austria.

#### References

- [1] G.T. Nikolov, V.C. Valchev, *Procedia Earth Planet. Sci.* 1 (2009) 1357–1361.
- [2] A. Gavrilović, D.M. Minić, L.D. Rafailović, P. Angerer, J. Wosik, A. Maričić, D.M. Minić, *J. Alloys Compd.* 504 (2010) 462–467.
- [3] D.M. Minić, A. Gavrilović, P. Angerer, D.G. Minić, A. Maričić, *J. Alloys Compd.* 476 (2009) 705–709.
- [4] D.M. Minić, A. Gavrilović, P. Angerer, D.G. Minić, A. Maričić, *J. Alloys Compd.* 482 (2009) 502–507.
- [5] J.D. Ayers, V.G. Harris, J.A. Sprague, W.T. Elam, H.N. Jones, *Acta Mater.* 46 (1998) 1861–1874.
- [6] K. Hono, D.H. Ping, M. Ohnuma, H. Onodera, *Acta Mater.* 47 (1999) 997–1006.
- [7] K. Hono, *Acta Mater.* 47 (1999) 3127–3145.
- [8] W. Martienssen, H. Warlimont, *Springer Handbook of Condensed Matter and Materials Data*, 1st ed., Springer, Berlin, Heidelberg, 2005.
- [9] Bruker AXS, TOPAS V3, General profile and structure analysis software for powder diffraction data, Karlsruhe, 2005.
- [10] M.M. Trexler, N.N. Thadhani, *Prog. Mater. Sci.* 55 (2010) 759–839.
- [11] W.S. Sun, M.X. Quan, *Mater. Lett.* 27 (1996) 101–105.